SIGNATURE OF TEMPORARY BURNING FRONT STALLING FROM A NON-PHOTOSPHERIC RADIUS EXPANSION DOUBLE-PEAKED BURST

Sudip Bhattacharyya[1,2], and Tod E. Strohmayer[2]

ABSTRACT

Non-photospheric-radius-expansion (non-PRE) double-peaked bursts may be explained in terms of spreading (and temporary stalling) of thermonuclear flames on the neutron star surface, as we argued in a previous study of a burst assuming polar ignition. Here we analyze Rossi X-ray Timing Explorer (RXTE) Proportional Counter Array (PCA) data of such a burst (but with a considerably different intensity profile from the previous one) from the low mass X-ray binary (LMXB) system 4U 1636–536, and show that this model can qualitatively explain the observed burst profile and spectral evolution, if we assume an off-polar, but high-latitude ignition, and burning front stalling at a higher latitude compared to that for the previous burst. The off-polar ignition can account for the millisecond period brightness oscillations detected from this burst. This is the first time oscillations have been seen from such a burst. Our model can qualitatively explain the oscillation amplitude measured during the first (weaker) peak, and the absence of oscillations during the second peak. The higher latitude front stalling facilitates the first clear detection of a signature of this stalling, which is the primary result of this work, and may be useful for understanding thermonuclear flame spreading on neutron stars.

Subject headings: accretion, accretion disks — relativity — stars: neutron — X-rays: binaries — X-rays: bursts — X-rays: individual (4U 1636–536)

1. Introduction

Thermonuclear burning of matter accumulated on the surfaces of accreting neutron stars produces type I X-ray bursts (Woosley, & Taam 1976; Lamb, & Lamb 1978). Although

[1]Department of Astronomy, University of Maryland at College Park, College Park, MD 20742-2421

[2]X-ray Astrophysics Lab, Exploration of the Universe Division, NASA's Goddard Space Flight Center, Greenbelt, MD 20771; sudip@milkyway.gsfc.nasa.gov, stroh@clarence.gsfc.nasa.gov

the lightcurves of most of these bursts have single-peaked structures, some of the strongest bursts from a given source show double-peaked profiles in higher energy bands. These can be explained in terms of photospheric radius expansion (PRE; due to radiation pressure), and subsequent contraction (Paczynski 1983). However, double-peaked structures are also seen in weak non-PRE bursts, and in such cases, these structures appear both in low and high energy bands. Such bursts have so far only been observed infrequently from a few sources (Sztajno et al. 1985). Until recently, models for these bursts did not simultaneously explain their intensity profiles, spectral evolution, X-ray emission area increase, and rarity (Fujimoto et al. 1988; Fisker, Thielemann, & Wiescher 2004; Regev, & Livio 1984; Melia, & Zylstra 1992). However, the recent model of Bhattacharyya & Strohmayer (2006), based on thermonuclear flame spreading on neutron stars, can qualitatively explain these properties. According to this model, such bursts are ignited close to a rotational pole (which explains the lack of millisecond period brightness oscillations), and then the burning front propagates (as a more or less ϕ-symmetric belt; ϕ is the azimuthal angle) towards the equator. As the front approaches the equator, it stalls for a few seconds before speeding up again into the opposite hemisphere. The stalling of the front allows the burning region to cool, and the luminosity to decrease. After a few seconds, as the flame starts spreading again, the increased temperature and emission area cause the luminosity to increase again, and hence a double-peaked structure appears in the burst profile. The physical reason for the temporary stalling of the front is still uncertain, though it might be caused by the accretion-induced pole-ward motion of burning shell matter (Bhattacharyya & Strohmayer 2006).

Our proposed model suggests that the non-PRE double-peaked bursts can be a useful tool to understand thermonuclear flame spreading on neutron star surfaces. Such an understanding may be important to constrain stellar surface parameters, as well as to model burst oscillations and their frequency evolution during burst rise (Bhattacharyya & Strohmayer 2005a; 2005b). Accurate modeling of burst oscillations has importance for constraining neutron star masses and radii, and hence the dense matter equation of state (EOS) (Bhattacharyya et al. 2005). In this Letter, analysing RXTE PCA data of a non-PRE double-peaked burst (with significantly different intensity profile from the burst analysed in Bhattacharyya & Strohmayer 2006) from the LMXB 4U 1636–536, (1) we report the discovery of oscillations for the first time from a non-PRE double-peaked burst, (2) we show that these oscillations can be accommodated in the spreading model, when high latitude but off-polar ignition is assumed (which still explains the rarity of these bursts), and most importantly, (3) we find a strong signature of temporary burning front stalling during this burst (which has been lacking in case of the Bhattacharyya & Strohmayer 2006 burst). We argue that these new results provide additional support for the idea that thermonuclear flame spreading can account for many of the features of non-PRE double-peaked bursts.

2. Data Analysis and Model Calculations

We analyze the RXTE PCA archival data of a double-peaked burst (Date of observation: Feb 28, 2002; ObsId: 60032-05-15-00) from 4U 1636–536. The second peak height ($\sim$ 5000 counts/s/PCU) is about three times larger than the first peak height (Fig. 1). This burst is weaker than PRE bursts observed from this source (Strohmayer et al. 1998). The similarity of the burst profile in different energy bands also indicates that this is not a PRE burst. We discovered oscillations (near the stellar spin frequency $\sim$ 582 Hz; Strohmayer & Markwardt 2002) during the first intensity peak, but not during the second. We calculated the power spectrum of 1 s of data during the first peak (Fig. 1). At 2 Hz resolution we find a peak power of 13.4 at the frequency $\sim$ 581 Hz. The probability of obtaining a power this high in a single trial from the expected χ^2 noise distribution (4 dof) is $\approx 2.18 \times 10^{-5}$. As the oscillations have been searched at the known frequency (which does not evolve by more than $\approx$ 6 Hz; Giles et al. 2002), multiplying by the number (= 3) of trials, we get a significance of 6.55×10^{-5}, which implies a $\sim 4\sigma$ detection. We also fit the phase-folded lightcurve of 1 s of data (marked with the vertical lines in Fig. 1) with a combined model of a sinusoid and a constant ($\chi^2/\mathrm{dof} = 10.67/13$, as opposed to $\chi^2/\mathrm{dof} = 25.13/15$ for a constant model), and find that the oscillation rms amplitude is 0.082 ± 0.022.

In order to track the burst spectral evolution, we break the burst profile into smaller time bins, and for each bin perform spectral fitting using a single temperature blackbody model (bbodyrad in XSPEC), as generally burst spectra are well fit by a blackbody. During the fitting, we fix the hydrogen column density $N_{\rm H}$ at a value 0.56×10^{22} cm^{-2} (Bhattacharyya & Strohmayer 2006). The fitting is performed after subtracting the persistent (i.e., preburst) emission from the emission during the burst. We show the time evolution of the best fit values of temperature and radius (calculated from the bbodyrad "normalization" parameter) in Fig. 2. This figure shows that these parameters are well correlated with the intensity profile, and the radius, which is a measure of the source emitting area, increases with time in a manner indicative of flame spreading. Here we note that some of the properties of this burst were also reported by Jonker et al. (2004), which they used only to conclude that this was not a PRE burst. The reduced χ^2 values for some of our time bins are high (> 1.5 for two out of 14 bins). We previously argued that this might result from temperature variations in the burning region at a given instant. The persistent emission may vary during the burst, which can have some effect on the inferred radius values derived from spectral fitting. To explore this possibility, we fit the background subtracted preburst emission with a model, and then fit the background subtracted burst spectra with the best fit values (but varying the normalization) of this same model, plus a blackbody. The resulting temporal evolutions of blackbody temperature and radius were found to be very similar to those shown in Fig. 2, providing additional confidence in the evolutionary tracks shown in this figure.

We explain the observed data using a model (involving flame spreading and its temporary stalling), which is very similar to that of Bhattacharyya & Strohmayer (2006; see § 1), except here we consider ignition at high latitudes (instead of polar ignition). This off-polar ignition gives rise to an expanding ϕ-asymmetric hot spot, which causes the oscillations during the first intensity peak. At a certain θ-location (θ is the polar angle), the θ-ward motion of the flame stalls temporarily, and its ϕ-ward motion quickly gives the burning region the shape of a ϕ-symmetric belt (that causes the disappearence of oscillations consistent with the observation), which then expands ϕ-symmetrically. The temporary stalling of the θ-ward motion, but not of the ϕ-ward motion, is consistent with the suggestion (Bhattacharyya & Strohmayer 2006) that this stalling is caused by accretion-induced pole-ward motion of burning shell matter, while the accretion is conducted via a disk, and hence is ϕ-symmetric. However, we model the observed burst intensity profile using a simplification, that the burst is ignited in a narrow ϕ-symmetric belt. This does not cause any error (within the context of our model) in the intensity profile after the maximum of the first peak (as at this time, stalling makes the hot spot ϕ-symmetric), and before this time, this simplified model approximately reproduces the intensity increase. We make this simplification for the following reasons. (1) The low signal to noise ratio data do not show any significant evolution of the oscillation amplitude or frequency. Therefore, an understanding of the burning region geometry evolution has to come from theoretical calculations. (2) A rigorous theoretical calculation of thermonuclear flame spreading considering all the main physical effects (e.g., that of magnetic field) is not available at the present time (but see Spitkovsky, Levin, & Ushomirsky 2002). However, we note that in reality there must be a ϕ-asymmetric burning region during the first peak rise in order to explain the oscillations. But this discrepancy will not be serious *as long as* the actual ϕ-asymmetric burning region can also approximately reproduce the first intensity peak. We examine this point now. From our model (Fig. 3), we find that at the time of the first intensity peak, the ϕ-symmetric burning region covers the θ-space from $\theta = 0°$ to $\theta = 40°$. A belt this wide, but with a ϕ-width of $\approx 260°$, produces an oscillation amplitude 0.072 ± 0.011 (consistent with the observed value), and an intensity that is within 9% of the maximum of the first intensity peak. Therefore, our simplified model can semi-quantitatively reproduce both the observed intensity and the oscillation amplitude simultaneously. Here we note that our assumed ϕ-elongated burning region is not unrealistic, as in this region the hot layers will puff up and "slip" in the ϕ-direction with respect to the stellar surface (in order to conserve angular momentum; Cumming & Bildsten 2000), causing a quicker spread of the flame in this direction (compared to the θ-direction) at a given latitude. We also note that as this effect affects only the ϕ-direction speed of the flame, our usage of Spitkovsy et al.'s (2002) ageostrophic flame speed (that does not include this effect) for θ-ward motion (see the next paragraph) is justified. However, this ϕ-elongated burning region geometry is only suggestive, and a more realistic geometry has to come from

(statistically) better data and rigorous theoretical studies.

As mentioned above, we calculate the intensity profile considering that the burst is ignited at a polar angle $\theta = \theta_c (= 10^\circ)$, and a narrow ϕ-symmetric belt expands in both directions with an angular speed $\dot{\theta}(\theta) = F(\theta)$, where $F(\theta) = 1/(t_{\rm total} \times \cos\theta)$ for $\theta \leq 90^\circ$, and $F(\theta) = 1/(t_{\rm total} \times \cos(180^\circ - \theta))$ for $\theta \geq 90^\circ$. Here $t_{\rm total}$ is the front propagation time (from a pole to the equator) without any stalling. Note that this particular expression of $F(\theta)$ (adopted from Spitkovsky et al. 2002; for weak turbulent viscosity) is *not* crucial for our qualitative results. We assume that the stalling of the front happens between the polar angles θ_1 and θ_2 (with $\theta_1 < \theta_2 < 90^\circ$): $\dot{\theta}(\theta)$ decreases linearly from $\theta = \theta_1$ to $\theta = \theta_m$, reaching a value $s/t_{\rm total}$, and then increases linearly up to $\theta = \theta_2$ reaching a value $F(\theta_2)$. Between $\theta = \theta_2$ and $\theta = 180^\circ$, we assume $\dot{\theta}(\theta) = F(\theta)$. To calculate the temperature of a given location at a certain time, we assume that after ignition of the fuel at that location, the temperature increases from $T_{\rm low}$ to $(T_{\rm low} + (0.99 \times (T_{\rm high} - T_{\rm low})))$ following the equation $T(t) = T_{\rm low} + (T_{\rm high} - T_{\rm low}) \times (1 - \exp(-t/t_{\rm rise}))$, and then decays exponentially with an e-folding time $t_{\rm decay}$. We compute lightcurves and spectra using this model (see Bhattacharyya & Strohmayer 2006 for details), considering Doppler, special relativistic, and general relativistic (gravitational redshift and light-bending in Schwarzschild spacetime) effects. In Fig. 3, for an example set of source parameter values, we show the evolutionary tracks of model intensity and spectral parameters (blackbody temperature and radius) that are qualitatively similar to the observed features of the double-peaked burst (Fig. 2). For example, the model reproduces the general shape of the observed intensity profile (including the $\sim 1/3$ ratio of first peak height to second peak height). For both data and model, the blackbody temperature starts from a high value, decreases up to the time when the intensity becomes minimum between the two peaks, increases up to the time when the intensity reaches the second peak, and declines after that. The inferred radius for both data and model starts from a low value, increases up to the time when the intensity reaches the first peak, remains almost unchanged up to the time when the intensity becomes minimum between the two peaks, increases again up to the time when the intensity reaches the second peak, and remains almost unchanged after that. The almost constant value of the inferred model radius during the decline of the first intensity peak (marked with the two vertical lines in Fig. 3) is due to the temporary stalling of the burning front. The occurrence of the same feature during the observed burst (see Fig. 2) is therefore a clear indication of front stalling. Note that for the emission from a localized hot spot, due to the lack of knowledge about the size and location of the spot, and the amount of light-bending (which depends on stellar parameters), we can not clearly interpret the inferred radius apart from suggesting that its square is approximately proportional to the burning region area. Therefore, we do not conclude anything directly from these inferred (from data) radii, but compute similar radii (using stellar and hot spot parameters as variables) from

the model, and then compare between these two sets. As we find the evidence of temporary front stalling from this comparison, we consider it to be strong. We note that the more gradual rise of the model burst peaks may be because of the delay between ignition at depth and emergence of the radiation (Bhattacharyya & Strohmayer 2006), and the simplification (i.e., a ϕ-symmetric ignition) of the model. The observed higher second peak temperature compared to that of the first peak (Fig. 2; which does not happen for the model) may be due to the slightly higher burst maximum temperature ($T_{\rm high}$) during the second peak than that just after the burst onset (while we do not consider such a $T_{\rm high}$-variation in the model). Such a temperature difference is not unrealistic, as for accretion via a disk, the lighter element hydrogen (as opposed to helium) is expected to spread more towards the pole. This would cause a higher hydrogen-to-helium ratio near the pole (than near the equator), and hence lower $T_{\rm high}$ value just after the burst onset (as the burst ignites at a high latitude). We also note that the model burst duration scales with the parameter $t_{\rm total}$, and hence can be adjusted by changing the value of this parameter.

3. Discussion and Conclusions

In this Letter we show that our simple model, based on thermonuclear flame spreading and its temporary stalling, can qualitatively reproduce the intensity and spectral profiles of a non-PRE double-peaked burst from 4U 1636-53. The burst studied here is different from the one described in a previous paper (Bhattacharyya & Strohmayer 2006) in the sense that the peaks of this burst have considerably different fluxes, while they were almost equal for the previous one. The observed radius profile of this burst is also different from that of the previous burst (Fig. 2). Moreover, this burst provides an additional challege to the flame spreading model in that one must account for the detection of oscillations in the first peak. In addition, although the general support for flame spreading and its temporary stalling comes from this burst, as well as from the previous burst, a clear (disentangled from other effects) evidence of front stalling has been lacking until this study, which we describe below. During the stalling, the inferred radius is not expected to change much (as the emission area does not), and this constancy in radius value should correlate with the decrease of the intensity and the temperature caused by the stalling (see § 1). Therefore, this constancy in between two clear increases (due to flame spreading) of radius values can give a very strong evidence of stalling (disentangled from other effects). Such a clear evidence was missing from the previous burst. This is because, for the previous burst, we had to consider a low latitude stalling (to reproduce the equal intensity peak heights), which made the constancy in radius due to stalling confused with the radius constancy in the later stage of spreading, as these two were almost connected (and the radius values were similar within error bars;

Fig. 1 of Bhattacharyya & Strohmayer 2006). This later radius constancy happened when the burning region expanded into the opposite hemisphere, and the front went out of the sight (and hence the visible source area did not increase much). But for the burst studied here, this evidence is present because of high latitude stalling (which is required to reproduce the observed asymmetric intensity profile). Therefore, this burst provides the first clearly disentangled signature of front stalling (see the pairs of vertical lines in Figs. 2 & 3). Our model can also explain the rarity of these bursts, as high-latitude ignition should be rare according to Spitkovsky et al. (2002; Bhattacharyya & Strohmayer 2006; Bhattacharyya et al. 2000). Moreover, our model prefers the slower front speed (for weak surface turbulent viscosity) of the two front propagation speed scenarios presented by Spitkovsky et al. (2002).

Our discovery of millisecond period brightness oscillations from the observed burst is the first such detection from a non-PRE double-peaked burst, and our model can qualitatively account for the observed rms amplitude, as well as the occurrence of these oscillations only during the first intensity peak. Our model also suggests that the details of the evolution of the burning region geometry can be obtained from the data (with better signal to noise ratio), that show significant oscillation amplitude and frequency evolution. However, we note that although the observed oscillations are consistent with our model involving thermonuclear flame spreading, the possibility that these oscillations have the same origin as that of burst tail oscillations can not be completely excluded. Therefore, to more firmly establish our model, as well as to understand the physics behind front stalling, it is essential to conduct rigorous fluid dynamical calculations and simulations, and to expand the sample of non-PRE double-peaked bursts by observing 4U 1636–536, and other similar sources for longer time periods with RXTE PCA and future larger area detectors.

We thank the referee for pointing out a discrepancy, and helping to improve the paper.

REFERENCES

Bhattacharyya, S., & Strohmayer, T. E. 2005a, ApJ, 634, L157.

Bhattacharyya, S., & Strohmayer, T. E. 2005b, submitted to ApJ.

Bhattacharyya, S., & Strohmayer, T. E. 2006, ApJ, 636, L121.

Bhattacharyya, S., Strohmayer, T. E., Miller, M. C., & Markwardt, C. B. 2005, ApJ, 619, 483.

Bhattacharyya, S., Thampan, A. V., Misra, R., & Datta, B. 2000, ApJ, 542, 473.

Cumming, A. & Bildsten, L. 2000, ApJ, 544, 453.

Fisker, J. L., Thielemann, F., & Wiescher, M. 2004, ApJ, 608, L61.

Fujimoto, M. Y., Sztajno, M., Lewin, W. H. G., & van Paradijs, J. 1988, A&A, 199, L9.

Giles, A. B., Hill, K. M., Strohmayer, T. E., & Cummings, N. 2002, ApJ, 568, 279.

Jonker, P. G. et al. 2004, MNRAS, 354, 666.

Lamb, D. Q., & Lamb, F. K. 1978, ApJ, 220, 291.

Melia, F., & Zylstra, G. J. 1992, ApJ, 398, L53.

Paczynski, B. 1983, ApJ, 276, 315.

Regev, O., & Livio, M. 1984, A&A, 134, 123.

Spitkovsky, A., Levin, Y., & Ushomirsky, G. 2002, ApJ, 566, 1018.

Sztajno, M. et al. 1985, ApJ, 299, 487.

Strohmayer, T. E., & Markwardt, C. B. 1999, ApJ, 516, L81.

Strohmayer, T. E., & Markwardt, C. B. 2002, ApJ, 577, 337.

Strohmayer, T. E., Zhang, W., Swank, J. H., White, N. E., & Lapidus, I. 1998, ApJ, 498, L135.

Woosley, S. E., & Taam, R. E. 1976, Nature, 263, 101.

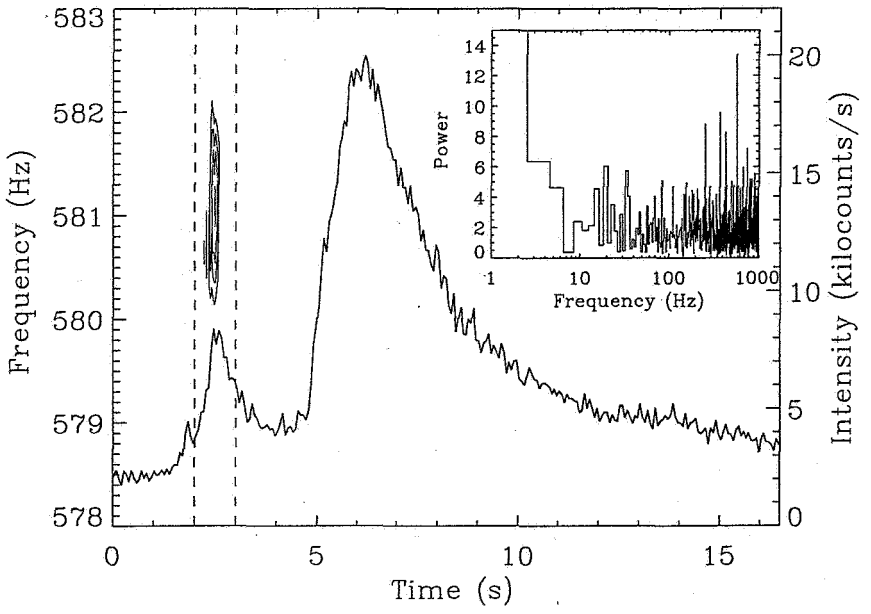

Fig. 1.— A non-PRE double-peaked burst from 4U 1636–536. The main panel shows the PCA count rate profile (four PCUs on). The inset panel shows the power spectrum of the 1 s interval (marked with vertical dashed lines in the main panel) during the first peak, rebinned to 2 Hz resolution. The peak near 581 Hz implies a significant signal power. Power contours using the dynamic power spectra (for 0.5 s duration at 0.03 s intervals) are shown in the main panel (Strohmayer & Markwardt 1999). Contours at power levels of 15, 18, 21, 25 are shown. These power contours show that oscillations occur only during the first intensity peak.

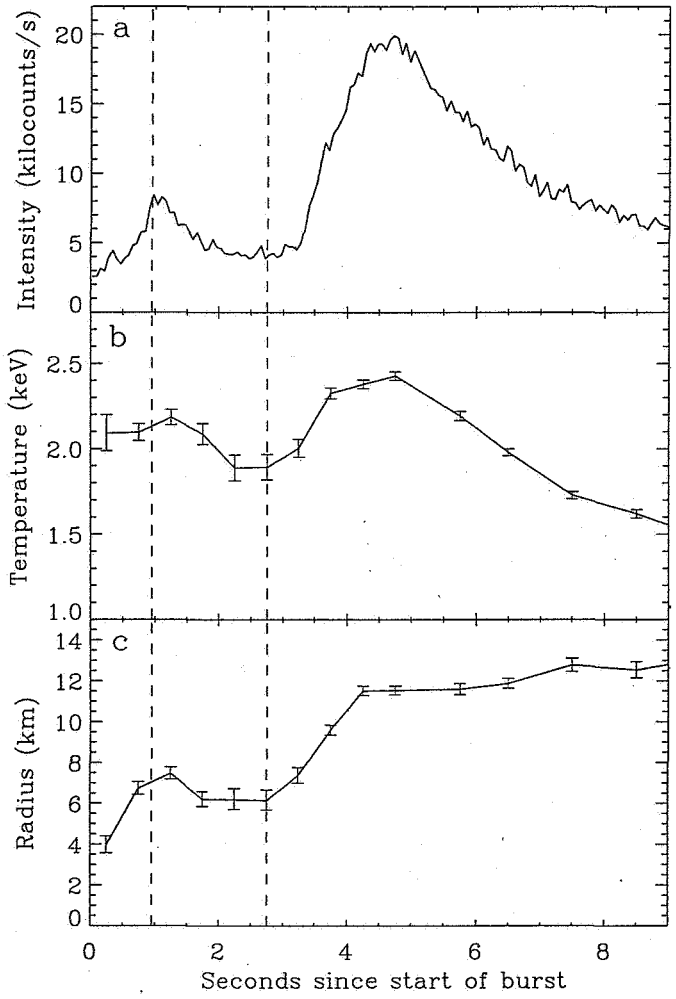

Fig. 2.— A non-PRE double-peaked burst from 4U 1636–536. Panel *a* gives the bolometric burst profile. Panels *b* & *c* show the time evolution of the blackbody temperature and the apparent radius (assuming 10 kpc source distance) of the emission area respectively, obtained by fitting the burst spectrum (persistent emission subtracted) with a single temperature blackbody model. The error bars are 1σ. Vertical dashed lines give the time interval in which the radius (and hence the source emission area) does not change, and the possible burning front stalling occurs.

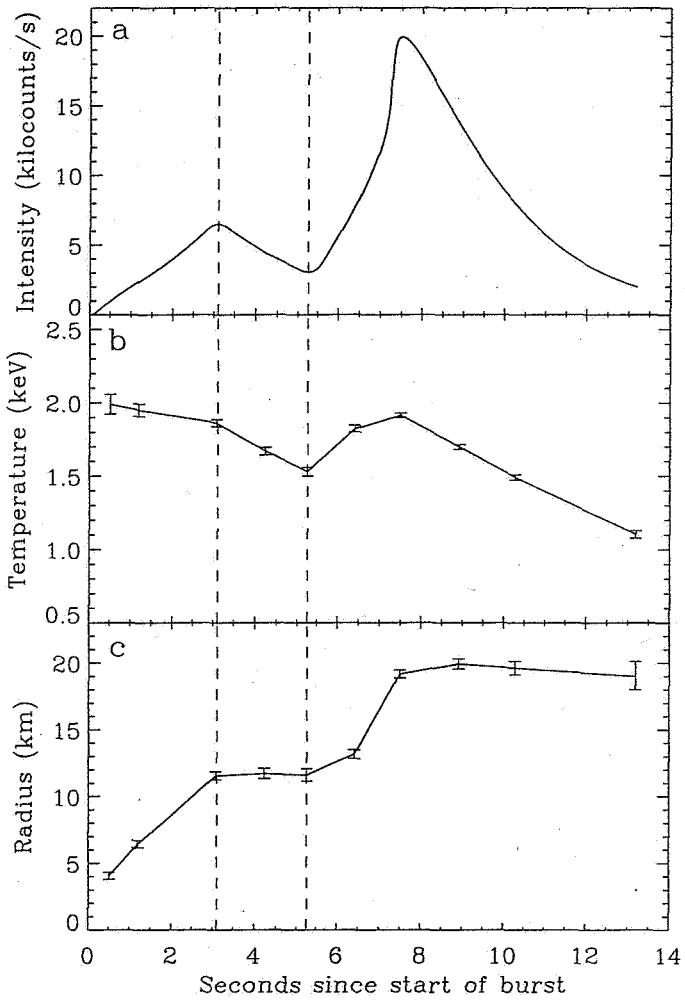

Fig. 3.— Model (convolved with a PCA response matrix) of the double-peaked burst: for all the panels, the burst is normalised so that its second intensity peak has the same count rate as that of the second peak of the observed burst. Panels are similar to those of Fig. 2. Model parameter values are the following: stellar mass $M = 1.5 M_{\odot}$, dimensionless stellar radius to mass ratio $R/M = 5.5$, stellar spin frequency $\nu_* = 582$ Hz, observer's inclination angle $i = 40°$, $\theta_c = 10°$, $\theta_1 = 40°$, $\theta_m = 43°$, $\theta_2 = 46°$, $s = 0.004$, $t_{\rm total} = 6$ s, $t_{\rm rise} = 0.05$ s, $t_{\rm decay} = 8$ s, $T_{\rm low} = 0.2$ keV, and $T_{\rm high} = 2.6$ keV (see text for the definitions of the parameters). The error bars are of 1σ size. Vertical dashed lines give the time interval, in which the radius (and hence the source emission area) does not change much, and the burning front stalling occurs.